

## Synthetic Ion Channel Based on Metal–Organic Polyhedra\*\*

Minseon Jung, Hyunuk Kim, Kangkyun Baek, and Kimoon Kim\*

The flow of ions in living cells, essential for them to survive, is regulated by ion channels. Studies of synthetic ion channels are important not only for the understanding of natural ion channels,<sup>[1]</sup> but also for applications such as in drug discovery<sup>[2]</sup> and sensors.<sup>[3]</sup> Since the first synthetic ion channels were reported in the early 1980s,<sup>[4]</sup> many synthetic ion channels and pores have been studied.<sup>[5–7]</sup> With one exception,<sup>[8]</sup> however, all the synthetic ion channels reported so far are made of organic molecules such as crown ethers,<sup>[6a,b]</sup> cyclic peptides,<sup>[6c]</sup> and rigid-rod  $\beta$ -barrels.<sup>[6d]</sup>

Nanosized three-dimensional (3D) metal–organic cages or metal–organic polyhedra (MOP) have been studied extensively in recent years.<sup>[9]</sup> MOP-18 (Figure 1), first reported by Yaghi and co-workers,<sup>[10]</sup> is one of the most

stable metal–organic cages and is readily synthesized by self-assembly from 5-dodecoxybenzene-1,3-dicarboxylic acid ( $5\text{-OC}_{12}\text{H}_{25}\text{-}m\text{BDC}$ ) and  $\text{Cu}(\text{CH}_3\text{CO}_2)_2\cdot\text{H}_2\text{O}$  at room temperature. The charge-neutral cuboctahedron core<sup>[11]</sup> (Figure S1 in the Supporting Information) built with 12 copper paddle-wheel units joined by 24  $m\text{BDC}$  linkers has a hydrophilic cavity with a diameter of  $13.8\text{ \AA}$ ,<sup>[10]</sup> which is accessible through 8 triangular and 6 square windows each with a diameter of  $3.8\text{ \AA}$  and  $6.6\text{ \AA}$ , respectively. The passages to the cavity are lined with the aromatic  $m\text{BDC}$  moieties (Figure 1). The overall size of the metal–organic cage including the long alkyl chains decorating the outside of the cage is approximately  $5\text{ nm}$ . Its rigid core with a large accessible cavity, lipophilic shell, and large enough size to span lipid bilayers prompted us to investigate the possibility of ion-channel formation of MOP-18 in lipid bilayers. Herein we report a synthetic ion channel formed with MOP-18 that transports proton and alkali metal ions across lipid membranes. To the best of our knowledge, it is the first synthetic ion channel based on 3D metal–organic cages.

The proton-transport activity of MOP-18 in lipid membranes was examined using EYPC-LUVs (egg yolk phosphatidylcholine–large unilamellar vesicles), which were prepared as described.<sup>[12]</sup> Incorporation of MOP-18 into the vesicle membrane was evidenced by a strong peak at  $1669\text{ cm}^{-1}$  in the FTIR spectrum corresponding to its carboxylate groups (Figure S2 in the Supporting Information). Proton transport across the membranes was assessed by the change in fluorescence intensity of the pH sensitive dye HPTS (8-hydroxypyrene-1,3,6-trisulfonate) entrapped inside the vesicles. A sudden generation of a pH gradient across the membranes by adding HCl solution to the extravesicular solution<sup>[13]</sup> resulted in immediate quenching of the fluorescence (Figure S3 in the Supporting Information), which supports the hypothesis that MOP-18 is involved in the proton transport across the membrane.

The alkali metal ion transport activity of MOP-18 was also assessed by fluorometry by using a well-established protocol.<sup>[6h]</sup> The transport activity of MOP-18 decreases in the order  $\text{Li}^+ \gg \text{Na}^+ > \text{K}^+ > \text{Rb}^+ > \text{Cs}^+$  (Figure 2), which follows Eisenman sequence XI,<sup>[1]</sup> suggesting that binding of the cations to the channel is more crucial than dehydration of the cations in the ion transport.<sup>[1,14]</sup> The initial rate of  $\text{Na}^+$  ion transport increases linearly with the mole fraction of MOP-18 (Figure S4 in the Supporting Information), which suggests that a single MOP-18 molecule constitutes the ion channel.

The ion-transport activity of MOP-18 in planar lipid bilayers was investigated by the voltage-clamp method.<sup>[15a]</sup> Homogeneous, long-lived single-channel currents were observed, as illustrated in Figure 3a for a typical current profile obtained at an applied voltage of  $+60\text{ mV}$  across the membrane separating symmetric  $2\text{ M KCl}$  solutions.<sup>[16]</sup> The

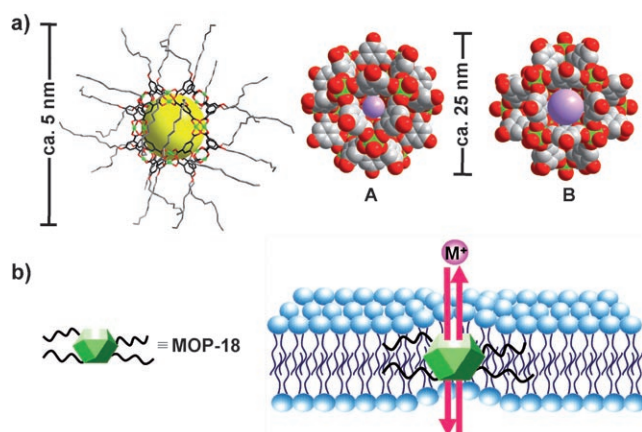


**Figure 1.** a) MOP-18 with a framework formula  $\text{Cu}_{24}(\text{5-OC}_{12}\text{H}_{25}\text{-}m\text{BDC})_{24}$  has a large cavity (yellow sphere, diameter  $13.8\text{ \AA}$ ). Triangular and square windows are shown as spheres (purple) that fit into the windows (diameter  $3.8\text{ \AA}$  for A and  $6.6\text{ \AA}$  for B) (see also Figure S1 in the Supporting Information). b) A schematic diagram for a synthetic ion channel formed by MOP-18 in lipid bilayers.

[\*] M. Jung, H. Kim, K. Baek, Prof. Dr. K. Kim  
National Creative Research Initiative Center for Smart Supramolecules and Department of Chemistry, Pohang University of Science and Technology, San 31 Hyoja-dong, Pohang 790-784 (Republic of Korea)  
Fax: (+82) 54-279-8129  
E-mail: kkim@postech.ac.kr  
Homepage: <http://css.postech.ac.kr>

[\*\*] We acknowledge the Creative Research Initiatives and BK21 Programs for support of this work. X-ray diffraction experiments with synchrotron radiation were performed at the Pohang Accelerator Laboratory (Beamline 6C1) supported by the MEST and Pohang University of Science and Technology.

Supporting information for this article is available on the WWW under <http://dx.doi.org/10.1002/anie.200802240>.

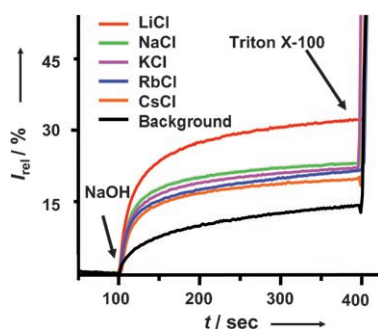


**Figure 2.** Changes in the fluorescence intensity ratio ( $I_{460}/I_{403}$ ) of HPTS associated with the alkali metal ion transport of MOP-18 in LUV as a function of time. Suspensions of EYPC-LUVs in a phosphate buffer were used (1.1 mM EYPC, 10 mM sodium phosphate, pH 6.4, 100 mM MCl: M =  $\text{Li}^+$ ,  $\text{Na}^+$ ,  $\text{K}^+$ ,  $\text{Rb}^+$ , and  $\text{Cs}^+$ ). MOP-18 (1 mol%) was incorporated into the vesicles at the hydration step (see the Experimental Section).

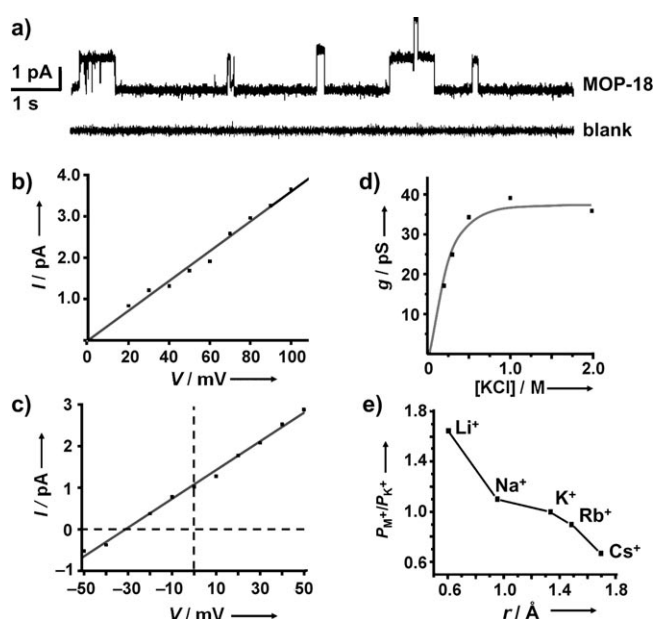


**Figure 3.** a) Typical current profile measured with and without MOP-18 at +60 mV in 2 M KCl. b) Single-channel  $I$ - $V$  profile of conductance with a linear curve fit for symmetric 2 M KCl and c) for asymmetric 2 → 0.25 M KCl (cis → trans). d) Single-channel conductance as a function of KCl concentration with a curve fit to the Michaelis-Menten equation. e) Permeability ratios for monovalent cations as a function of their Pauling radii. For each experiment, a membrane composed of 1:1 PS (phosphatidylserine)/PE (phosphatidylethanolamine) was used. MOP-18 (1 mol%) solution was painted onto an aperture of the “cup” before voltage-clamp recording (see the Experimental Section).

current-voltage plot in Figure 3b revealed ohmic behavior of the ion channel formed by MOP-18, as expected. From the slope, a single-channel conductance of 36 pS was calculated for the membrane in symmetric 2 M KCl, which is comparable to that of gramicidin.<sup>[17]</sup> The MOP-18 channel prefers cations over anions. The current-voltage relationship (Figure 3c) obtained with a salt gradient (0.25 to 2 M) showed a reversal potential  $V_r = -31$  mV, from which a permeability ratio  $P_{\text{K}^+}/P_{\text{Cl}^-} = 5.5$  was calculated by using the Goldman-Hodgkin-

Katz equation.<sup>[1]</sup> The single-channel conductance showed saturation behavior as the  $\text{K}^+$  ion concentration increases (Figure 3d).<sup>[15]</sup> Michaelis-Menten analysis revealed that the expected blockage by  $\text{K}^+$  occurred at an inhibitory cation concentration  $\text{IC}_{50} = 0.22$  M with a maximal single-channel conductance of  $g_{\text{max}} = 44$  pS. The inner channel diameter can be estimated from the single-channel conductance by using Hille's equation. The corrected Hille diameter  $d_{\text{Hille}} = 5.4$  Å was obtained from the estimated conductance at 100 mM KCl (Figure 3d),<sup>[15,18]</sup> which is larger than the size of the triangular windows (3.8 Å) but smaller than that of the square windows (6.6 Å). This result seems to suggest that the MOP-18 channel utilizes both windows as ion passages.<sup>[16]</sup>

The cation selectivity from reversal potentials obtained under  $\text{M}^+/\text{K}^+$  gradients also follows the order  $\text{Li}^+ \gg \text{Na}^+ > \text{K}^+ > \text{Rb}^+ > \text{Cs}^+$  (Figure 3e), which is consistent with the result from fluorometry described above. The selectivity sequence (Eisenman sequence XI) with an exceptional selectivity for  $\text{Li}^+$  makes the present ion channel quite unique, as most synthetic ion channels follow Eisenman sequences I-IV (weak field-strength sequences).<sup>[5c]</sup> Although there is no direct evidence, the observed cation selectivity seems to suggest that the interaction<sup>[19]</sup> between cations and the  $\pi$  system of the aromatic rings lining the portals to the cavity plays a crucial role in the ion transport. Further studies to elucidate the mechanism of the ion transport in the MOP-18 channel are in progress.

In summary, we have reported the first synthetic ion channel based on well-defined metal-organic polyhedra that can transport proton and alkali-metal ions across lipid membranes. The large windows may also allow small molecules to pass through, which is currently under investigation. The size and chemical environment of the cavity and windows of the MOP is expected to be easily tuned by modification of the organic ligand constituting the framework. Other metal-organic cages such as Fujita's,<sup>[9a]</sup> if properly modified to be incorporated into lipid bilayers, can also be used as synthetic ion channels and pores.<sup>[8]</sup> The novel ion-channel system with easy synthesis, rigid structure, and tunability of the size and chemical environment of pores may also find useful applications in many areas including detection and separation of ions and small molecules as well as in catalysis.

## Experimental Section

MOP-18 was synthesized according to a literature method<sup>[10a]</sup> and recrystallized from acetonitrile and toluene. The structure of the compound was confirmed by single-crystal X-ray crystallography.

Preparation of vesicles for alkali metal ion transport: EYPC (1.7 mL) in chloroform ( $20 \text{ mg mL}^{-1}$ ) was dried in a flask with a rotary evaporator and then further dried under high vacuum for 1 day. After addition of phosphate buffer solution containing HPTS (2 mL, 100 mM NaCl, 10 mM phosphate,  $10 \mu\text{M}$  HPTS, pH 6.4) and MOP-18 (1 mol%) in THF (50  $\mu\text{L}$ ), the lipid film was hydrated by sonication at  $60^\circ\text{C}$ . The suspension was extruded to yield large unilamellar vesicles (LUVs) with a diameter of approximately 200 nm. The vesicle suspension was passed through a Sephadex G-50 column to remove untrapped dye and further dialyzed against phosphate buffer solution by using a membrane (molecular weight cutoff: 3500) for 4 h to prepare a vesicle stock solution.

Ratiometric fluorescence experiments: The emission of HPTS at 510 nm was monitored at two different excitation wavelengths (460 nm and 403 nm) simultaneously. The vesicle stock solution (200  $\mu$ L, pH 6.4) containing HPTS prepared as described above was mixed with MCl phosphate buffer solution (1800  $\mu$ L, 100 mM MCl: M =  $\text{Li}^+$ ,  $\text{Na}^+$ ,  $\text{K}^+$ ,  $\text{Rb}^+$ ,  $\text{Cs}^+$ , 10 mM sodium phosphate, pH 6.4) in a fluorescence cuvette. During the experiment, 0.5 M NaOH solution (40  $\mu$ L) was added through an injection port to cause an increase in pH value from 6.4 to 7.4 in the extravesicular buffer solution. The maximal changes in the dye emission were obtained at the end of each experiment by lysis of the vesicles with 5% Triton X-100. The final transport trace was obtained as a ratio of the emission intensities ( $I_{460}/I_{403}$ ) and normalized.

Planar bilayer lipid membrane voltage-clamp experiments: A solution of phosphatidylethanolamine (PE, 20  $\mu$ g) and phosphatidylserine (PS, 20  $\mu$ g) in *n*-decane (20  $\mu$ L) was painted around a 200  $\mu$ m diameter aperture of the bilayer "cup". For incorporation of MOP-18, two chambers were initially filled with 0.25–2 M KCl in 10 mM Tris-HEPES (Tris-HEPES = tris(hydroxymethyl)aminomethane/2-[4-(2-hydroxyethyl)-1-piperazinyl]ethanesulfonic acid). A solution of MOP-18 (5  $\mu$ g), PS (20  $\mu$ g), and PE (20  $\mu$ g) in *n*-decane (20  $\mu$ L) was painted onto an aperture of the "cup" and gently stirred. The *cis* chamber was held at the voltage control side, while the *trans* side was held at virtual ground. The conductance of channels was estimated from the slope of *IV* curve. Data calculations were performed according to a literature method.<sup>[15a]</sup>

Received: May 13, 2008

Published online: June 24, 2008

**Keywords:**  $\pi$  interactions · ion channels · nanostructures · self-assembly · supramolecular chemistry

- [1] B. Hille, *Ionic Channels of Excitable Membranes*, 3rd ed., Sinauer Associates, Inc., Sunderland, MA, 2001.
- [2] a) S. Fernandez-Lopez, H.-S. Kim, E. C. Choi, M. Delgado, J. R. Granja, A. Khasanov, K. Kraehenbuehl, G. Long, D. A. Weinberger, K. M. Wilkoxen, M. R. Ghadiri, *Nature* **2001**, 412, 452–456; b) V. Sidorov, F. W. Kotch, J. L. Kueber, Y.-F. Lam, J. T. Davis, *J. Am. Chem. Soc.* **2003**, 125, 2840–2841.
- [3] a) L.-Q. Gu, O. Braha, S. Conlan, S. Cheley, H. Bayley, *Nature* **1999**, 398, 686–690; b) B. A. Cornell, V. L. B. Braach-Maksyitis, L. G. King, P. D. J. Osman, B. Raguse, L. Wiczorek, R. J. Race, *Nature* **1997**, 387, 580–583; c) S. Howorka, S. Cheley, H. Bayley, *Nat. Biotechnol.* **2001**, 19, 636–639; d) S. Litvinchuk, H. Tanaka, T. Miyatake, D. Pasini, T. Tanaka, G. Bollot, J. Mareda, S. Matile, *Nat. Mater.* **2007**, 6, 576–580; e) G. Das, P. Talukdar, S. Matile, *Science* **2002**, 298, 1600–1602.
- [4] a) I. Tabushi, Y. Kuroda, K. Yokota, *Tetrahedron Lett.* **1982**, 23, 4601–4604; b) A. J. M. Van Beijnen, R. J. M. Nolte, J. W. Zwikker, W. Drenth, *Recl. Trav. Chim. Pays-Bas* **1982**, 101, 409–410.
- [5] Reviews: a) G. W. Gokel, A. Mukhopadhyay, *Chem. Soc. Rev.* **2001**, 30, 274–286; b) S. Matile, A. Som, N. Sordé, *Tetrahedron* **2004**, 60, 6405–6435; c) A. L. Sisson, M. R. Shah, S. Bhosale, S. Matile, *Chem. Soc. Rev.* **2006**, 35, 1269–1286; d) J. T. Davis, *Angew. Chem.* **2004**, 116, 684–716; *Angew. Chem. Int. Ed.* **2004**, 43, 668–698; e) T. M. Fyles, *Chem. Soc. Rev.* **2007**, 36, 335–347; f) A. P. Davis, D. N. Sheppard, B. D. Smith, *Chem. Soc. Rev.* **2007**, 36, 348–357.
- [6] Classic examples: a) O. Murillo, S. Watanabe, A. Nakano, G. W. Gokel, *J. Am. Chem. Soc.* **1995**, 117, 7665–7679; b) T. M. Fyles, T. D. James, K. C. Kaye, *J. Am. Chem. Soc.* **1993**, 115, 12315–12321; c) M. R. Ghadiri, J. R. Granja, L. K. Buehler, *Nature* **1994**, 369, 301–304; d) N. Sakai, K. C. Brennan, L. A. Weiss, S. Matile, *J. Am. Chem. Soc.* **1997**, 119, 8726–8727; e) Y. Kobuke, K. Ueda, M. Sokabe, *J. Am. Chem. Soc.* **1992**, 114, 7618–7622; f) M. J. Pregel, L. Jullien, J. Canceille, L. Lacombe, J.-M. Lehn, *J. Chem. Soc. Perkin Trans. 2* **1995**, 417–426; g) M. Merritt, M. Lanier, G. Deng, S. L. Regen, *J. Am. Chem. Soc.* **1998**, 120, 8494–8501; h) V. Sidorov, F. W. Kotch, G. Abdrakhmanova, R. Mizani, J. C. Fetting, J. T. Davis, *J. Am. Chem. Soc.* **2002**, 124, 2267–2278.
- [7] Recent examples: a) W. M. Leevy, J. E. Huettner, R. Pajewski, P. Schlesinger, G. W. Gokel, *J. Am. Chem. Soc.* **2004**, 126, 15747–15753; b) M. G. J. Ten Cate, M. Crego-Calama, D. N. Reinhoudt, *J. Am. Chem. Soc.* **2004**, 126, 10840–10841; c) W.-H. Chen, M. Nishikawa, S.-D. Tan, M. Yamamura, A. Satake, Y. Kobuke, *Chem. Commun.* **2004**, 872–873; d) V. Janout, B. S. L. Jing, Regen, *J. Am. Chem. Soc.* **2005**, 127, 15862–15870; e) S. Bhosale, A. L. Sisson, P. Talukdar, A. Fürstenberg, N. Banerji, E. Vauthey, G. Bollot, J. Mareda, C. Röger, F. Würthner, N. Sakai, S. Matile, *Science* **2006**, 313, 84–86; f) A. Cazacu, C. Tong, A. van der Lee, T. M. Fyles, N. Barboiu, *J. Am. Chem. Soc.* **2006**, 128, 9541–9548; g) Y. J. Jeon, H. Kim, S. Jon, N. Selvapalam, D. H. Oh, I. Seo, C.-S. Park, S. R. Jung, D.-S. Koh, K. Kim, *J. Am. Chem. Soc.* **2004**, 126, 15944–15945; h) M. S. Kaucher, W. A. Harrell, Jr., J. T. Davis, *J. Am. Chem. Soc.* **2006**, 128, 38–39.
- [8] An ion channel formed by a lipophilic ethylenediamine palladium(II) complex was reported recently. However, the channel-forming structure and ion-transfer mechanism are not clear: T. M. Fyles, C. Tong, *New J. Chem.* **2007**, 31, 655–661.
- [9] a) M. Fujita, M. Tominaga, A. Hori, B. Therrien, *Acc. Chem. Res.* **2005**, 38, 369–380; b) S. T. Seidel, P. J. Stang, *Acc. Chem. Res.* **2002**, 35, 972–983; c) D. L. Caulder, K. N. Raymond, *Acc. Chem. Res.* **1999**, 32, 975–982; d) L. R. MacGillivray, J. L. Atwood, *Angew. Chem.* **1999**, 111, 1080–1096; *Angew. Chem. Int. Ed.* **1999**, 38, 1018–1033.
- [10] a) H. Furukawa, J. Kim, K. E. Plass, O. M. Yaghi, *J. Am. Chem. Soc.* **2006**, 128, 8398–8399; b) M. Eddaoudi, J. Kim, J. B. Wachter, H. K. Chae, M. O’Keeffe, O. M. Yaghi, *J. Am. Chem. Soc.* **2001**, 123, 4368–4369.
- [11] The core structure of MOP-18 was originally described as great rhombicuboctahedron. However, we prefer an alternative description, cuboctahedron consisting of eight triangular and six square faces based on “node and spacer” approach with the paddle-wheel unit as a node and mBDC as a spacer.
- [12] K. Kano, J. H. Fendler, *Biochim. Biophys. Acta Biomembr.* **1978**, 509, 289–299.
- [13] No structure change of MOP-18 upon external pH changes during the experiments (from pH 7.0 to 5.5 for proton transfer or from pH 6.4 to 7.4 for alkali metal ion transfer) is apparent by UV/Vis spectroscopy.
- [14] a) G. Owsianik, K. Talavera, T. Voets, B. Nilius, *Annu. Rev. Physiol.* **2006**, 68, 685–717; b) G. Eisenman, R. Horn, *J. Membr. Biol.* **1983**, 76, 197–225.
- [15] a) N. Sakai, Y. Kamikawa, M. Nishii, T. Matsuoka, T. Kato, S. Matile, *J. Am. Chem. Soc.* **2006**, 128, 2218–2219; b) Z. Qu, H. C. Hartzell, *J. Gen. Physiol.* **2000**, 116, 825–844.
- [16] Close inspection of Figure 3a and the histogram of the current profile (Figure S5 in the Supporting Information) revealed that there are two types of channels with significantly different single-channel currents, which may be because the cuboctahedron core of MOP-18 has two different types of windows, as described above, leading to two different types of ion channels. Further studies to elucidate the details are in progress.
- [17] Under similar conditions, gramicidin shows a conductance of 26 pS. See p. 365 of reference [1].
- [18] O. S. Smart, J. Breed, G. R. Smith, M. S. P. Sansom, *Biophys. J.* **1997**, 72, 1109–1126.
- [19] a) D. A. Dougherty, *Science* **1996**, 271, 163–168; b) J. C. Ma, D. A. Dougherty, *Chem. Rev.* **1997**, 97, 1303–1324.